ISSN 0965-545X, Polymer Science, Ser. A, 2011, Vol. 53, No. 8, pp. 655–665. © Pleiades Publishing, Ltd., 2011.
Original Russian Text © I.A. Budagovsky, A.S. Zolot'ko, V.N. Ochkin, M.P. Smayev, S.A. Shvetsov, A.Yu. Bobrovsky, N.I. Boiko, V.P. Shibaev, M.I. Barnik, 2011, published in Vysokomolekulyarnye Soedineniya, Ser. A, 2011, Vol. 53, No. 8, pp. 1337–1348.

Orientational Optical Nonlinearity of Nematic Liquid Crystals Induced by High-Molecular-Mass Azo-Containing Compounds[1]

I. A. Budagovsky[a], A. S. Zolot'ko[a], V. N. Ochkin[a], M. P. Smayev[a], S. A. Shvetsov[a], A. Yu. Bobrovsky[b], N. I. Boiko[b], V. P. Shibaev[b], and M. I. Barnik[c]

[a] *Lebedev Physical Institute, Russian Academy of Sciences, Leninskii pr. 53, Moscow, 119991 Russia*
[b] *Moscow State University, Faculty of Chemistry, Moscow, 119991 Russia*
[c] *Shubnikov Institute of Crystallography, Russian Academy of Sciences, Leninskii pr. 59, Moscow, 119333 Russia*
e-mail: zolotko@lebedev.ru

Abstract—Processes of light-induced reorientation of nematic liquid-crystalline molecules induced by the addition of low concentrations (0.1–2.0 wt %) of comb-shaped polymers and carbosilane dendrimers containing azobenzene fragments are studied. When the molecular structure of the above compounds becomes more complicated, the induced orientational nonlinearity increases. The introduction of 2G and 3G dendrimers into a nematic has for the first time made it possible to visualize and study a purely optical first-order Freedericksz transition in the field of a linearly polarized wave.

DOI: 10.1134/S0965545X11080025

INTRODUCTION

The light-induced reorientation of molecules entails changes in the refractive index of a medium and various nonlinear optical phenomena, such as self-focusing and self-defocusing, wavefront conjugation, optical bistability, and formation of solitons etc. This phenomenon can be used for data recording, control over propagation of light beams, optical modulation, and other applications. The phenomena of optical reorientation are most pronounced for a "soft matter," whose simplest representatives are nematic liquid crystals (NLCs).

In liquid crystals, the nematic phase is produced by rodlike molecules: Owing to the action of intermolecular forces, they align primarily in one direction that is locally characterized by a unit vector, director **n** [1, 2]. The NLC director can be easily rotated by an external low-frequency electrical field. This phenomenon serves as a basis for diverse applications of NLCs. A similar effect is observed for light fields [3–6]. A light beam passing through a layer of a transparent NLC rotates director **n** and aligns it along the direction parallel to the direction of light field **E**, thus increasing the refractive index of an extraordinary wave. The corresponding ("positive") orientational optical nonlinearity of the NLC is nine orders of magnitude higher than the Kerr nonlinearity of conventional liquids [4]. The mechanism of optical orientation in nonabsorbing NLCs is related to the action of light field **E** on dipoles induced in the NLC molecules by the same field. The torque acting on molecules of a nematic matrix and normalized to the unit volume of the NLC has the form

$$\mathbf{\Gamma} = \frac{\Delta\varepsilon |A|^2}{8\pi}(\mathbf{ne})[\mathbf{ne}], \quad (1)$$

where $\Delta\varepsilon$ is the dielectric anisotropy at the light frequency, A is the light-field amplitude, and **e** is the light-polarization unit vector.

When a nematic matrix is doped with dye molecules, orientational optical nonlinearity can increase by three orders of magnitude (when the concentration of the additive is ~1 wt %) [7]. In the-doped NLCs, the director can rotate both parallel and perpendicularly to the light-field direction. In the second case, the refractive index of the extraordinary wave decreases. ("Negative" nonlinearity is observed [8].)

The mechanisms leading to the light-induced rotation of the director in the absorbing NLCs cannot be considered indisputable, and several models of this phenomenon are known [9–14]. However, it is common knowledge that the rotation of the director requires the development of an ensemble of excited dye molecules whose orientational distribution is asymmetric with respect to the director [7]. The torque acting on the director of the absorbing NLC can be described by a relationship that is similar to Eq. (1):

[1] This work was supported by the Russian Foundation for Basic Research (project nos. 11-02-01315 and 11-03-01046) and the federal target program Scientific and Educational Specialists of Innovation Russia (State Contract no. 02.740.11.0447).

$$\mathbf{\Gamma} = \frac{\Delta\varepsilon_{eff}|A|^2}{8\pi}(\mathbf{ne})[\mathbf{ne}] \quad (2)$$

Instead of $\Delta\varepsilon$, this relationship includes $\Delta\varepsilon_{eff}$ which is referred to as the effective dielectric anisotropy ($\Delta\varepsilon_{eff}$ can be positive or negative). The nonlinear optical response of the absorbing NLCs can be characterized by the ratio of the effective dielectric anisotropy and the true dielectric anisotropy, $\eta = \Delta\varepsilon_{eff}/\Delta\varepsilon$, which may be called the *nonlinearity enhancement factor*.

Of special interest are azo-doped LC systems whose configurations of molecules can undergo light-induced changes. For example, it was found [15] that, for such systems, the sign of nonlinearity (and, correspondingly, the direction of the light-induced reorientation of the director) depends on angle γ between the light field and the director: The nonlinearity is positive when γ is lower than a certain critical level $\gamma < \gamma_{cr}$ and is negative at $\gamma > \gamma_{cr}$. This dependence can be explained as follows: First, trans and cis isomers of the azo dye generate negative and positive nonlinearity in the nematic matrix, respectively; and, second, the ratio of concentrations $u = c_{trans}/c_{cis}$ of these isomers in the light field depends on angle γ [16]. The latter circumstance is provided by different order parameters of the isomers. (The order parameter of the trans isomers is higher because of their elongated shape.) As a result, as γ increases, the average cross section of the optical absorption of trans isomers, $\sigma_{trans}(\gamma)$, decreases at a higher rate than the cross section of the absorption of cis isomers, $\sigma_{cis}(\gamma)$. In the strong field $u \sim \sigma_{cis}(\gamma)/\sigma_{trans}(\gamma)$, and the sign of the nonlinearity can reverse as the fraction of trans isomers increases.

As absorbing molecules that enhance nonlinearity, dopants based on low-molecular-mass dyes are traditionally used. At the same time, high-molecular-mass compounds seem to be promising candidates for the optical orientation of liquid crystals, because, compared to low-molecular-mass compounds, they have some parameters that are crucial for the light-induced director reorientation. For example, macromolecules have higher rotational diffusion times and moments of inertia (a circumstance that should assist the development of an ensemble of excited molecules with an angular distribution asymmetric with respect to the director). Moreover, the spatial distribution of the absorbing fragments in the nematic matrix can be strongly inhomogeneous, in contrast to the spatial distribution of the low-molecular-mass dyes.

Pioneering observations over orientational nonlinearity induced in the NLCs by a high-molecular-mass compound (the polymer MEH-PPV) were reported in [17]. The negative orientational nonlinearity of this LC system is an order of magnitude higher than the nonlinearity of the undoped nematic matrix.

This current paper presents results from the investigation of the orientational action of light on LC systems doped with comb-shaped polymers and various generations of dendrimers containing azobenzene fragments. The experimental samples and experimental procedures are described, and experimental results from previous studies of the LC systems containing comb-shaped polymers [14, 18, 19] and dendrimers [19–21] are revisited. One section is devoted to the light-induced first-order Freedericksz transition [21–23] due to the use of dendrimers.

EXPERIMENTAL SAMPLES AND PROCEDURE

As a nematic matrix, ZhKM-1277 liquid crystalline material (a mixture of biphenyls and esters, Research Institute of Organic Intermediaries and Dyes, Russia) was used. ZhKM-1277 can produce a nematic mesophase in the broad temperature interval −20 to +60°C and has a positive dielectric anisotropy ($\Delta\varepsilon = 12.1$ at a frequency of $\nu = 1$ kHz). The refractive indexes of extraordinary and ordinary waves are $n_{||} = 1.71$ and $n_{\perp} = 1.52$, respectively ($\lambda = 589$ nm).

Comb-shaped copolymers, 1G and 5G homodendrimers, and statistical 2G–4G codendrimers are used as azobenzene-containing high-molecular-mass dopants. To gain comparative data on the parameters of nonlinearity induced by high-molecular-mass dopants, experiments were performed for low-molecular-mass dyes whose structure is similar to the structure of "absorbing" azobenzene fragments of polymers and dendrimers.

The structural formulas of comb-shaped copolymers P-1 ($M = 4.7 \times 10^4$) and P-2 ($M = 7 \times 10^3$) are presented below.

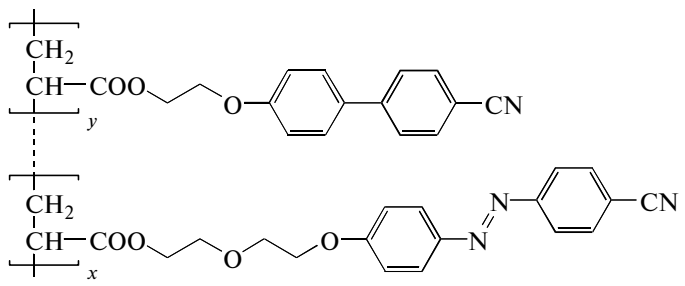

($x = 60\%$, $y = 40\%$);

P-1

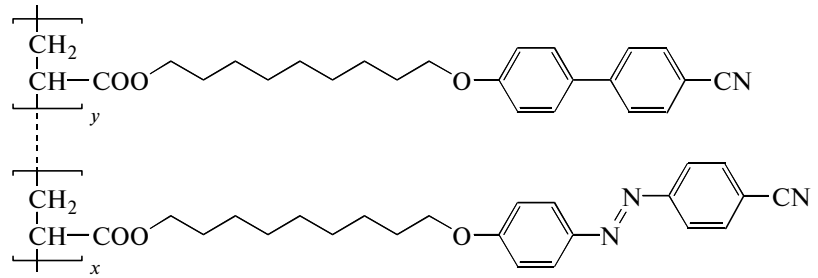

($x = 40\%$, $y = 60\%$).

P-2

The polymers contain cyanobiphenyl and azobenzene fragments attached to the alkyl chain by oxyaliphatic (P-1) and aliphatic spacers (P-2) of different lengths.

The structural formula of the used azo dye AD-1, which is similar to side azo fragments of the polymers, is presented below.

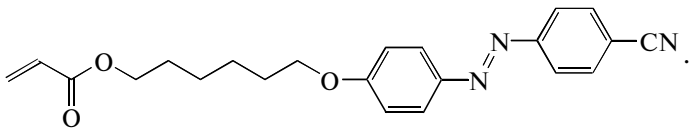

Figure 1 presents the molecular structures of 1G and 5G homodendrimers containing azobenzene terminal fragments and of the corresponding low-molecular-mass azo dye (AD-2). The synthesis, phase behavior, and photo-optical characteristics of the above compounds in isotropic solutions and as thin films were described in [24]. Figure 2 shows the structures of 2G, 3G, and 4G codendrimers containing azobenzene and aliphatic terminal fragments, which are randomly distributed on the dendrite surface. Their synthesis and characteristics were described in [25]. The weight concentration of azobenzene-containing polymers and dendrimers in the nematic matrix varied from 0.1 to 2.0%.

For all the studied azo compounds, the absorption maxima lie in the UV spectral interval. In the blue–green interval (440–550 nm), the absorption of the compounds monotonically decreases as the light wavelength increases. All LC mixtures feature marked dichroism. For example, for a 0.5% solution of P-1 in the ZhKM-1277 nematic matrix, the absorption coefficients are the following: $\alpha_{\parallel} = 51, 43, 33, 14$ cm^{-1} and $\alpha_{\perp} = 13, 11, 8, 3$ cm^{-1} at wavelengths of $\lambda = 458, 473, 488$, and 515 nm, respectively. The same values of the absorption coefficients were obtained for the ZhKM-1277 + 0.3 AD-1 sample containing nearly the same concentration of azo fragments. For ZhKM-1277 doped with the 4G dendrimer (0.15%), the absorption coefficients at a wavelength of $\lambda = 473$ nm were $\alpha_{\parallel} = 20$ cm^{-1} and $\alpha_{\perp} = 10$ cm^{-1}.

In our experiments, we used plane–parallel 100-μ-thick cells with a current-conducting layer (ITO); the cells were filled with the LC material. The studies were performed for planarly and homeotropically aligned LC cells. To produce a planar alignment, glasses were covered with thin (~50 nm) polyimide layers that were rubbed in opposite directions. In the homeotropic cells, chromium stearyl chloride was used as an aligning agent. The quality of the oriented cells was tested on a POLAM-213 polarization microscope.

The optical orientation in the LC systems was studied via the method of aberrational self-phase modulation of a light beam [19, 26, 27]. As an example, Fig. 3a shows the case of normal light incidence on the planarly oriented cell with negative nonlinearity. An extraordinary polarized beam with plane wavefront WF_0 is focused into a cuvette containing a liquid crystal. Laser-beam intensity I_0 in the transverse cross section has a Gaussian profile; hence, a light-induced change in the refractive index of the extraordinary wavefront is maximum along the light-beam axis (the dotted line in Fig. 3). This change leads to a bell-shaped of wavefront WF_1: its central part "runs away" from peripheral parts owing to a decrease in the refractive index. At the deformed wavefront, it is possible to define pairs of rays $\mathbf{k}_1$ and $\mathbf{k}_2$ with the same deviation from the beam axis. The interference of these rays leads to the formation of a set of concentric rings in the far region that are visible on a screen.

The number of aberration rings, N, is related to the thickness-averaged changes in the refractive index of the extraordinary wave through the simple relationship

$$|\Delta n| = N\lambda\cos\beta/L, \quad (3)$$

where L is the thickness of the LC cell, β is the light refraction angle.

The character of the changes in the transversal distribution of intensity in the ring pattern that are due to the shift of the LC cell relative to the light-beam axis makes it possible to define the aberration self-action

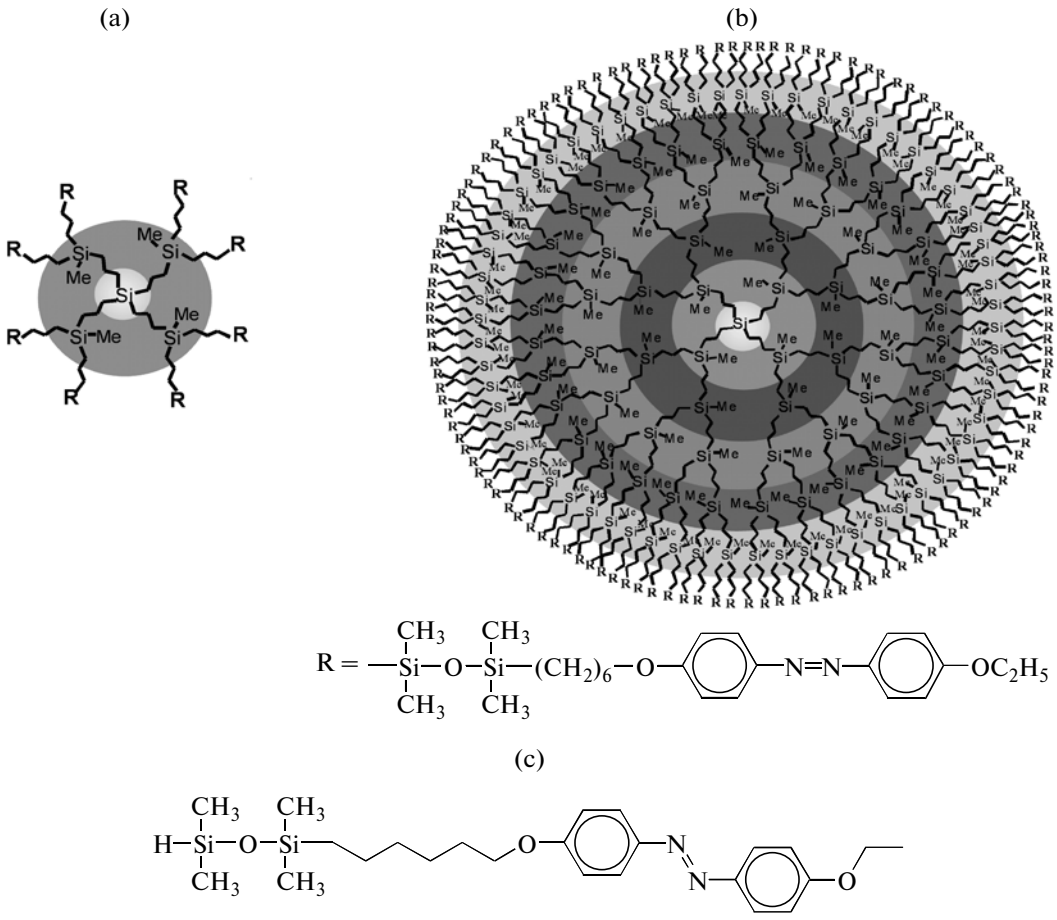

Fig. 1. (a) 1G and (b) 5G homodendrimers containing azobenzene terminal groups and (c) the azobenzene-containing low-molecular-mass analog AD-1 of the terminal group of dendrimers.

sign (an increase in the refractive index corresponds to the self-focusing of the beam, while a decrease in the refractive index corresponds to self-defocusing) [27]. In the case of the steady-state aberration pattern, the most intense ray, the axial ray, corresponds to wavefront point *A* (Fig. 3a). The times of formation and relaxation of the deformed director field are tens of seconds; hence, when a cuvette is swiftly shifted upward, the axial ray passing through point *B* (Fig. 3b) deviates under the action of the refractive-index gradient. In the case of the negative nonlinearity, the lower part of the ring pattern is brightened; in the case of the positive nonlinearity, the upper part of the aberration pattern is brightened.

Figure 4 shows the scheme of the experimental setup. As illumination sources, ILA-120 (λ = 458, 476, 488, and 515 nm) and LASOS (515 nm) argon lasers and an LCS-DTL-364 solid-state laser (473 nm) were used. A horizontally polarized light beam was focused on the sample through a lens with a focal length of f = 18 cm. The polarization plane of the light beam was rotated with a double Fresnel rhomb. The LC layer plane was vertical, and unperturbed director $\mathbf{n}_0$ lay in the horizontal plane. The angle of light incidence onto a crystal, α, can be varied via the rotation of a cuvette containing NLC around a vertical axis. For the described geometry of experiments in the homeotropic and planar cells, an extraordinary light wave was generated. An alternating voltage (ν = 3 kHz) from an MXG-9802A (METEX) generator could be applied to the cell. The aberration pattern induced in the transverse cross section of the light beam that was passed through the NLC layer was visualized on a screen.

INTERACTION OF LIGHT WITH NLC DOPED WITH COMB-SHAPED POLYMERS

The irradiation of the NLC samples containing copolymers or azo dye AD-1 leads to the development of a characteristic set of concentric aberration rings. This pattern is provided by reorientation of the director because its times of formation and relaxation ("collapse" as the light-beam power decreases) are tens of seconds. The sign of self-action shows that, for the polymer-doped homeotropic and planar samples, as well as for the homeotropically aligned sample con-

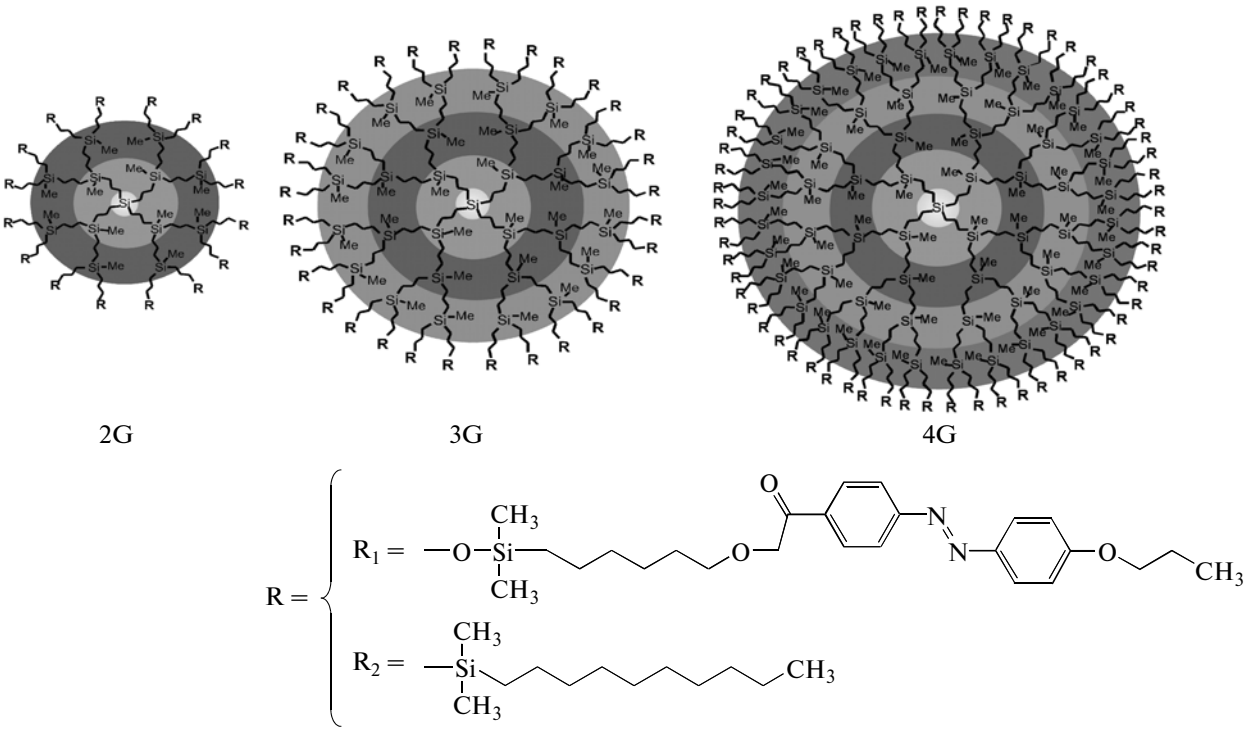

Fig. 2. 2G, 3G, and 4G codendrimers with statistically distributed aliphatic and azobenzene terminal fragments.

taining AD-1, self-defocusing of the light beam occurs (negative nonlinearity; NLC director **n** is aligned perpendicularly to the direction of light field **E**). In the case of the AD-1 doped planar crystal, the light beam undergoes self-focusing (positive nonlinearity; the NLC director is aligned along the field **E**).

Figure 5 shows the thickness-averaged changes in refractive index Δn plotted against light-beam power P for the planar samples. As P increases, $|\Delta n|$ monotonically increases and approaches its saturation level; for comb-shaped polymers P-1 (curves *1*, *4*) and P-2 (curve *2*), the orientational nonlinearity is much higher (at a lower power, a higher self-induced refractive index is attained) than that of low-molecular-mass dye AD-1 (curve *3*). For normal light incidence (curve *4*), the director reorientation shows a threshold character (P_{th} = 1.5 mW), as is typical of the light-induced Freedericksz transition. At high power P, the maximum change in refractive index $|\Delta n|$ in the saturation region approaches $|\Delta n_{sat}| = 0.2$. This result indicates a nearly complete reorientation of the director perpendicular to the light field.

In the case of normal light incidence onto homeotropic samples and on a planar crystal doped with AD-1, light self-action does not come into play. This behavior suggests negative nonlinearity for homeotropic samples and positive nonlinearity for the planar sample. During oblique light incidence onto homeotropically aligned samples beyond the saturation interval, $|\Delta n|$ for the LC system containing polymer P-1 is ~5 and ~10 times higher than those for the LC systems containing polymer P-2 and "free" molecules of azo dye AD-1.

Therefore, the polymers feature negative nonlinearity, irrespective of the angle γ between the light field and the director of the liquid crystal. For low-molecular-mass dye AD-1, nonlinearity reverses its sign: As γ increases (on passage from the planar alignment to the homeotropic alignment), positive nonlinearity becomes negative. As was mentioned in the introduction, this mode of nonlinearity was earlier observed for other low-molecular-mass azo compounds. Note also that, with a decrease in the length of a spacer joining an azo benzene group and a polymer chain, the orientational susceptibility of the LC system increases.

A difference between polymers and a low-molecular-mass dye is also evident when planar NLCs are exposed to a low-frequency field (Fig. 6). In the case of ZhKM-1277 + 0.5% P-1 (curve *1*) and ZhKM-1277 + 0.5% P-2, as voltage U increases, self-defocusing of the light beam occurs. During the application of a low-frequency voltage to the crystal doped with the AD-1 molecules (curve *2*), the sign of self-action reverses. In the homeotropic NLCs, irrespective of the nature of a dopant, the external field suppresses deformation of the director field; as a result, the number of self-defocusing rings monotonically decreases.

The experiments performed on polymer P-1 showed that the efficacy of the orientational action of light increases as polymer concentration c_p increases and the light wavelength decreases (i.e., the absorption

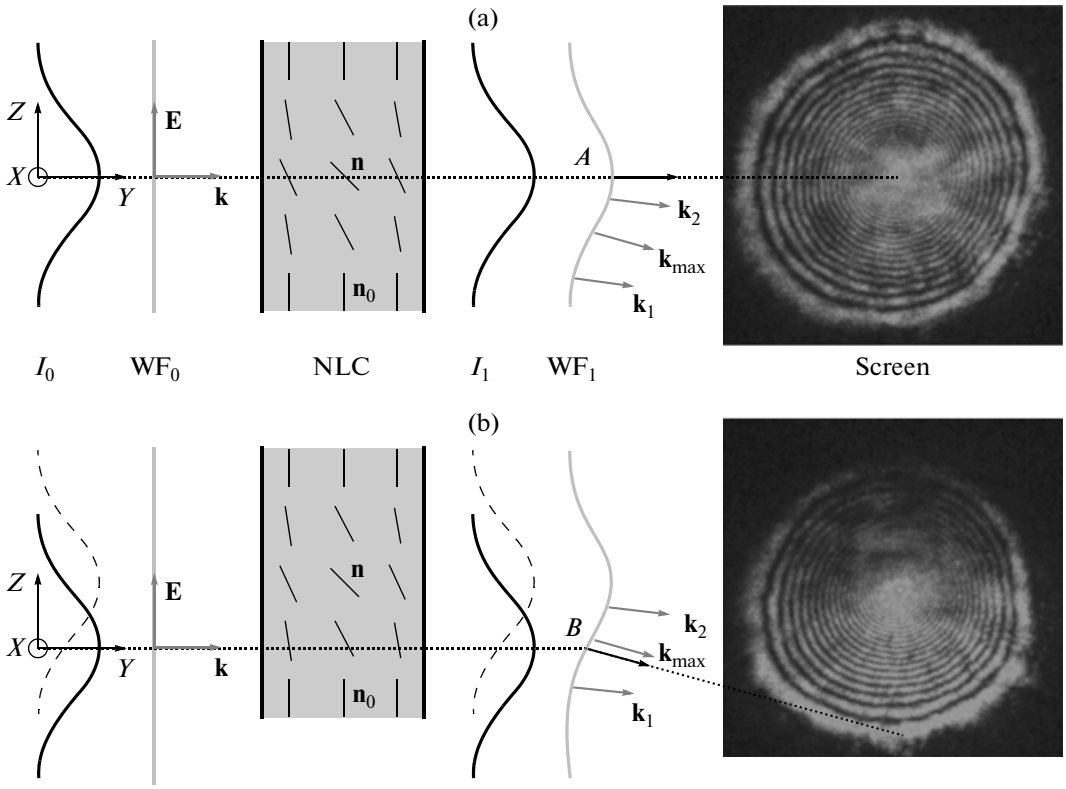

Fig. 3. (a) Formation of the aberration pattern in a beam after its passage through the NLC layer and (b) determination of the self-action sign. See text for explanations.

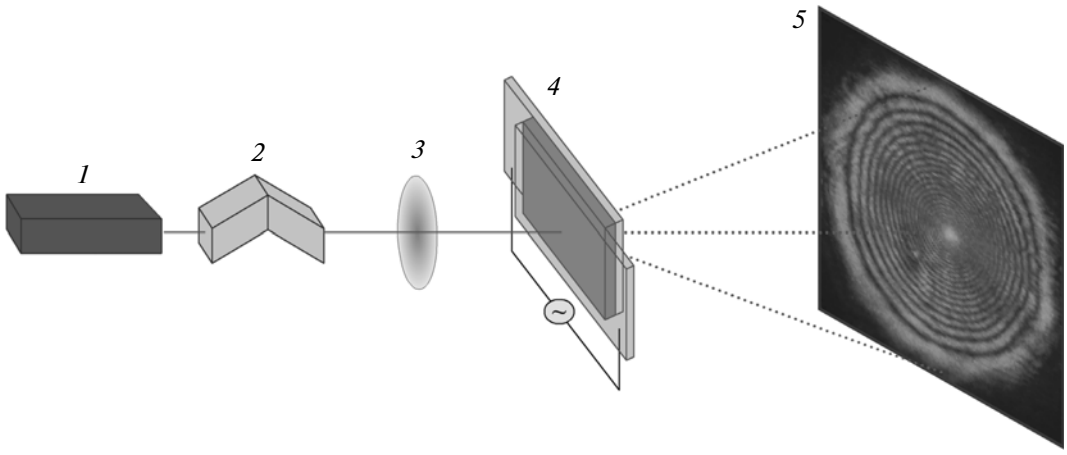

Fig. 4. Scheme of the experimental setup: (*1*) laser, (*2*) double Fresnel rhomb, (*3*) lens, (*4*) NLC, and (*5*) screen.

increases). For example, the threshold power of the director reorientation decreases by a factor of 12 (λ = 473 nm) when c_p increases from 0.1 to 2% and by a factor of 3 when the wavelength decreases from 515 to 476 nm.

To estimate the factor of nonlinearity enhancement, η, of the LC systems doped with polymer P-1 and dye AD-1, the values of power required for the same nonlinear optical response (the number of aberration rings) were compared. In the case of different signs of nonlinearity, the results for the samples with different alignments were compared. For the oblique light incidence (λ = 473 nm), η = 10 and −12.5 for the planar and homeotropic ZhKM-1277 + 0.3% AD-1 samples, respectively, and η = −30 for planar and homeotropic the ZhKM-1277 + 0.1% P-1 samples.

Let us compare the efficiency of optical reorientation induced by polymer P-1 and other absorbing

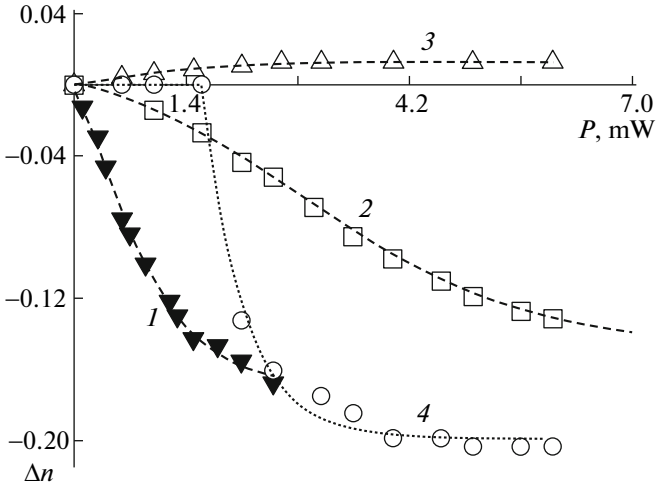

Fig. 5. Changes in refractive index Δn for an extraordinary wave plotted against light-beam power P (λ = 473 nm) after light beam passage through planarly oriented ZhKM-1277 samples containing (*1*, *4*) 0.5% polymer P-1, (*2*) 0.5% polymer P-2, and (*3*) 0.3% AD-1 dye. Curves *1–3* were obtained during oblique light wave incidence ($\alpha = 50°$); curve *4* was obtained under normal light incidence ($\alpha = 0°$).

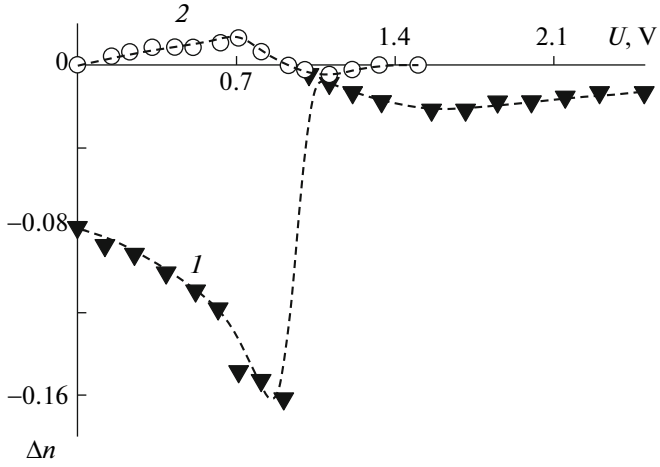

Fig. 6. Changes in refractive index Δn for an extraordinary wave (λ = 473 nm, P = 1 mW, $\alpha = 40°$) plotted against low-frequency (ν = 3 kHz) voltage U for the planarly oriented samples based on (*1*) ZhKM-1277 + 0.5% P-1 and (*2*) ZhKM-1277 + 0.3% AD-1.

dopants. The factor of nonlinearity enhancement, η, is proportional to the concentration of the dopant; hence, the nonlinear optical response can be reasonably characterized by $\eta_\alpha = \eta/(\alpha_\parallel + 2\alpha_\perp)$, which is proportional to the ratio between η and absorption $\alpha_{av} = (\alpha_\parallel + 2\alpha_\perp)/3$ averaged over the director orientations. For the oblique incidence of light with a wavelength of λ = 473 nm and for ZhKM-1277 + 0.1% P-1, $\eta = -30$ corresponds to $\eta_\alpha = -2.3$ cm. To our knowledge, by its absolute value, the nonlinearity parameter $\eta_\alpha = -2.3$ exceeds all known values both for negative nonlinearity ($\eta_\alpha = -0.05$ cm; calculations according to the data reported in [8] for anthraquinone dye D4) and for positive nonlinearity (η_α = 0.8 cm; calculations according to the data reported in [28] for oligothiophene TR5).

INTERACTION OF LIGHT WITH THE NLC DOPED WITH DENDRIMERS

As in the case of the comb-shaped polymers, when samples doped with homodendrimers and azo benzene dye AD-2 are irradiated with light, the aberration pattern depends on the nature of reorientation of the director. The sign of self-action suggests that, for low-molecular-mass dye AD-2 and a 1G dendrimer, nonlinearity alternates in sign: Nonlinearity is positive in the planar sample and negative in the homeotropic sample (Fig. 7). For the 5G dendrimer, nonlinearity is negative for any geometry of interaction between the light field and the director. In the case of normal light incidence, the threshold Freedericksz transition occurs (Fig. 7b, curve *4*).

The sign-alternating character of nonlinearity induced by dye AD-2 and a 1G dendrimer manifests itself also in the dependence of the refractive index on the external electrical field (Fig. 8).

As follows from Fig. 7a, the induced negative nonlinearity normalized by the dopant concentration increases in the order AD-2 ≥ 1G ≥ 5G as the molecular structure becomes more complicated.

The measurements of the dependence of the self-action of a light beam on the rotation angle of the polarization plane, $\varphi = 0°$ (from the polarization direction of the extraordinary wave and the perpendicular polarization direction of the ordinary wave $\varphi = 90°$), during oblique light incidence ($\alpha = 50°$) show that the nonlinearity changes in sign from positive to negative at a certain critical level ($\varphi_{cr} = 41°$ for AD-2 and 22° for 1G). These results and the relationship derived in terms of the theory of sign-alternating nonlinearity [27] make it possible to calculate critical angle γ between the light-field direction and the director; this angle is 47° for AD-2 and 34° for 1G.

For both planar and homeotropic samples, the action of light on the NLC containing 2G, 3G, and 4G codendrimers leads to negative nonlinearity that increases with the generation number (Fig. 9). The electrical field likewise does not change the sign of nonlinearity (Fig. 10).

FIRST-ORDER ORIENTATIONAL TRANSITIONS

The Freedericksz transitions under a low-frequency electrical field are traditionally second-order orientational transitions, and director rotation angle ψ is a continuous function of the field. The exception is the first-order transition in the field parallel to the LC

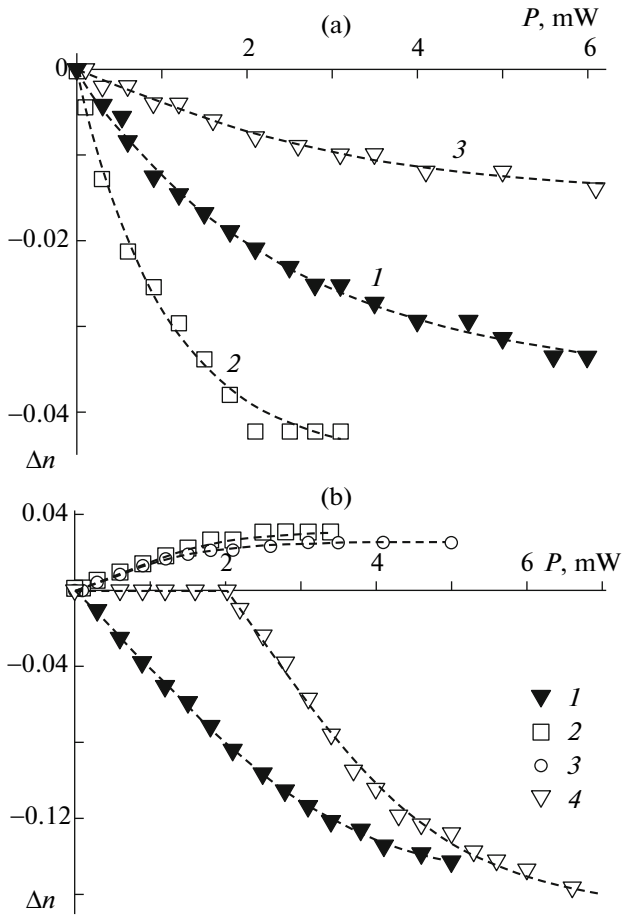

Fig. 7. Changes in refractive index Δn for the extraordinary wave plotted against light-beam power P ($\lambda = 473$ nm, $\alpha = 50°$) after passage of the light beam through (a) homeotropic and (b) planarly oriented ZhKM-1277 samples containing (*1*, *4*) 0.1% 5G dendrimer, (*2*) 0.5% 1G dendrimer, and (*3*) 0.5% AD-2 dye. Curves *1*–*3* were obtained during oblique light wave incidence ($\alpha = 50°$); curve *4* was obtained during normal light incidence ($\alpha = 0°$).

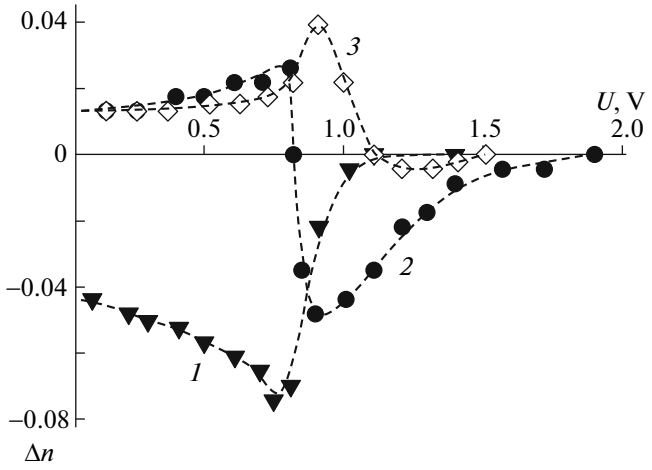

Fig. 8. Changes in refractive index Δn for the extraordinary wave ($\lambda = 473$ nm, $\alpha = 40°$) plotted against low-frequency ($\nu = 3$ kHz) voltage U for planarly oriented samples: (*1*) ZhKM-1277 + 0.1% 5G dendrimer, (*2*) ZhKM-1277 + 0.5% 1G dendrimer, and (*3*) ZhKM-1277 + 0.5% AD-2.

layer [29] that is characterized by a jump in ψ. Theoretical studies [30, 31] have predicted light-induced first-order transitions in a linearly polarized light wave at high optical anisotropy, which provides a feedback between the director rotation and the electrical field of the wave. However, the light-induced first-order Freedericksz transitions are observed only in the presence of an additional stabilizing low-frequency field [32–34].

The use of NLCs doped with azo compounds allows observation of the light-induced first-order transition without any additional effect. This possibility is due to the dependence of enhancement factor η on angle γ between the light-field direction and the director, which serves as an additional feedback between the director rotation and torque (Eq. (2)). This relationship becomes most pronounced in the sign-alternating nonlinearity; however, in this case, the threshold reorientation is not observed, because normal incidence of the light wave onto a homeotropic or a planar cell stabilizes the director field. The threshold reorientation occurs, for example, during normal light incidence onto the planar NLC with negative nonlinearity. As was mentioned in the introduction, because of the rotation of the director in this geometry, the concentration of trans isomers should increase and, thus, nonlinearity enhancement factor η, which is negative, should increase in absolute value. As a result, at the threshold power of the light-induced Freedericksz transition, the stable deformed state of the director field can arise and the light-induced reorientation of the director becomes the first-order orientational transition.

Figure 11 presents the light-induced refractive index plotted against power of the normally incident light beam for the planarly oriented NLCs doped with 2G, 3G, and 4G dendrimers. As follows from Fig. 11, all samples feature threshold Freedericksz transitions and the threshold values decrease as the generation number increases; this circumstance corresponds to an increase in nonlinearity. In this case, for the 2G and 3G dendrimers, the Freedericksz transition is a first-order orientational transition: As the light-beam power increases up to certain level P_1 (for the 2G dendrimer, $P_1 = 24$ mW), the reorientation of the director and the concomitant decrease in the refractive index change abruptly, rather than gradually, as in the case of the 4G dendrimer. This transition is accompanied by bistability: As power P decreases, the back transition occurs at a power of $P_2 < P_1$ (for the 2G dendrimer, $P_2 = 15$ mW). The relative width of the bistability region is $\Delta_P = (P_1 - P_2)/P_1 = 0.38$. For the third-generation dendrimers, $\Delta_P = 0.1$.

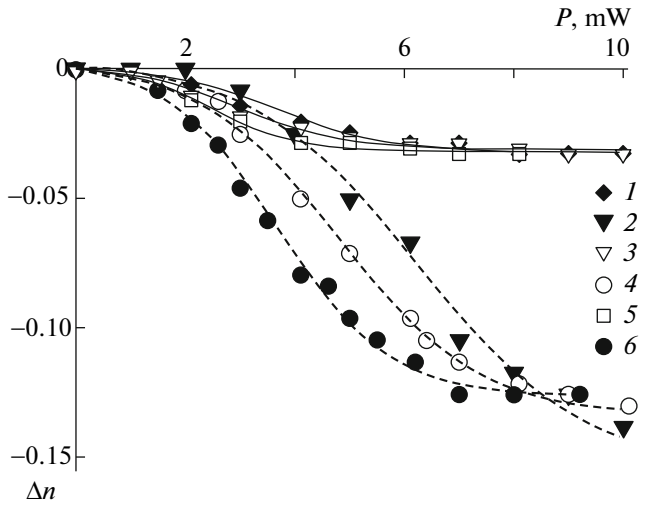

Fig. 9. Changes in refractive index Δn for the extraordinary wave plotted against light-beam power P (λ = 473 nm) after light beam passage through (*1*, *3*, *5*) homeotropically and (*2*, *4*, *6*) planarly oriented ZhKM-1277 samples containing (*1*, *2*) 0.15% 2G dendrimer, (*3*, *4*) 0.15% 3G dendrimer, and (*5*, *6*) 0.15% 4G dendrimer.

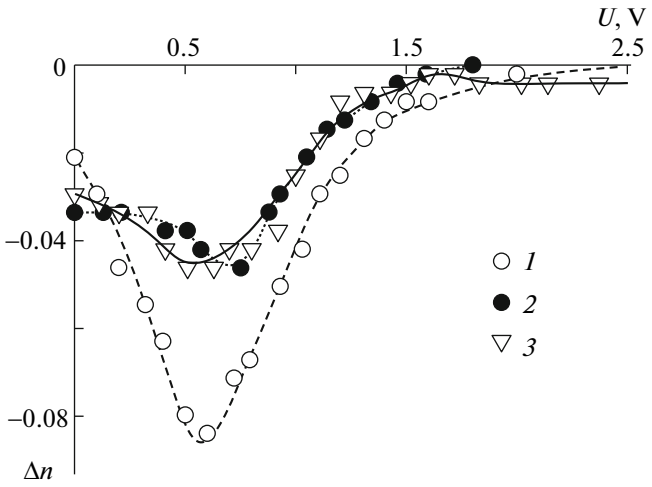

Fig. 10. Changes in refractive index Δn for the extraordinary wave plotted against low-frequency (ν = 3 kHz) voltage U for the planarly oriented samples: (*1*) ZhKM-1277 + 0.15% 2G dendrimer, (*2*) ZhKM-1277 + 0.15% 3G dendrimer, and (*3*) ZhKM-1277 + 0.15% 4G dendrimer: P = (*1*) 5, (*2*) 3, and (*3*) 2.6 mW.

The first-order transition was likewise observed during changes in the voltage applied to the NLCs irradiated with a light wave.

The theory of the light-induced first-order transition [23] considers the reorientation of the director under torque acting on the induced dipoles (according to Eq. (1), this parameter is controlled by optical anisotropy $\Delta\varepsilon$) and the torque of intermolecular forces induced by excitation of dopant molecules (estimated via expression 2 from parameter $\Delta\varepsilon_{eff}$). The sum $\Delta\varepsilon_{tot} = \Delta\varepsilon + \Delta\varepsilon_{eff}$ is approximated by the simple expression

$$\Delta\varepsilon_{tot}(\psi) = -\Delta\varepsilon_{eff}^{(0)}(1 + m\sin^2\psi), \qquad (4)$$

where ψ is the director rotation angle and $\Delta\varepsilon_{eff}^{(0)}$ and m are positive parameters. In terms of the continuum models for NLCs, the steady-state values of rotation angle ψ_0 of the director at the center of the LC layer are described by the following equation:

$$\psi_0 = \delta_P\left[\left(1 + \frac{m}{2}\right)J_1(2\psi_0) - \frac{m}{4}J_1(4\psi_0)\right] \qquad (5)$$

Here, $J_1(x)$ is the Bessel function, $\delta_P = \dfrac{\Delta\varepsilon_{eff}^{(0)}|A|^2 L^2}{8\pi^3 K}$ is the dimensionless light-wave power density (δ_P = 1 corresponds to the transition threshold), and K is the elastic Frank constant. Figure 12 presents the solutions of Eq. (5) at different parameters m. At $m > 0.8$, the Freedericksz transition becomes a first-order transition that is accompanied by bistability of the director field. As m increases, the interval of bistability widens. Parameter m is estimated from the experimental data on the width of the bistability region, Δ_P; for 2G and 3G, the values of m are 3.2 and 1.4, respectively. For the 4G dendrimer, the bistability region is absent; hence, parameter m should be lower than 0.8. Therefore, as the generation number of dendrimers increases, the dependence of effective anisotropy on the angle between the light-field direction and the director (which depends on parameter m) becomes

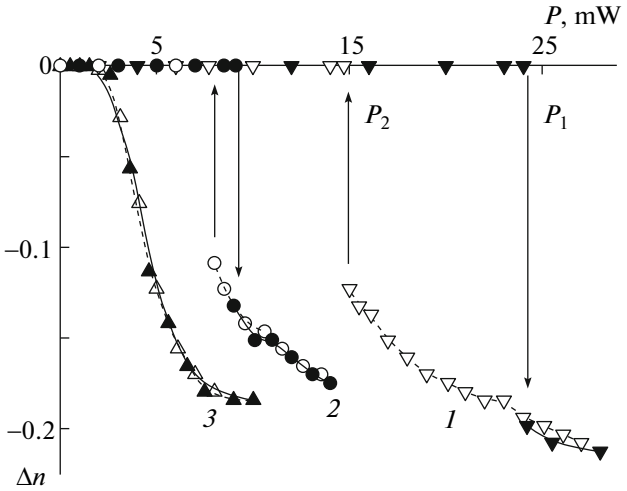

Fig. 11. Changes in refractive index Δn for the extraordinary wave P plotted against light-beam power P (λ = 473 nm, $\alpha = 0°$) after light-beam passage through the planarly oriented samples based on ZhKM-1277 containing (*1*) 0.15% 2G dendrimer, (*2*) 0.15% 3G dendrimer, and (*3*) 0.15% 3G dendrimer: (closed symbols) increases and (open symbols) decreases in light-beam power P.

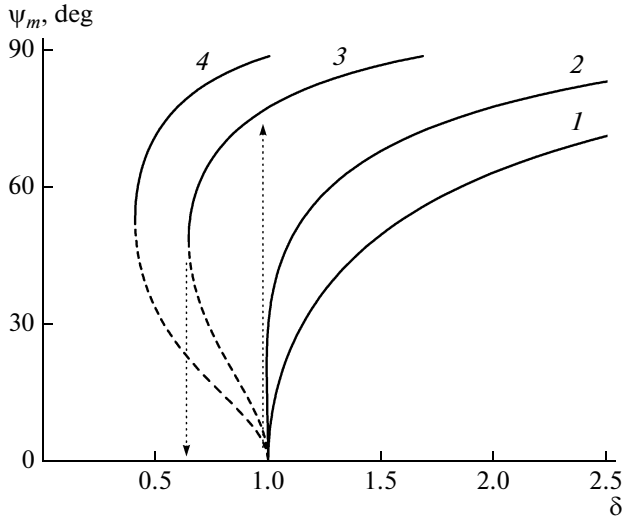

Fig. 12. Theoretical dependences of the rotation angle ψ_m of the director on dimensionless light-wave intensity δ at values of parameter m of (*1*) 0, (*2*) 0.8, (*3*) 3, and (*4*) 6. Curve *2* corresponds to the onset of bistability: (solid lines) stable solutions and (dashed lines) unstable solutions.

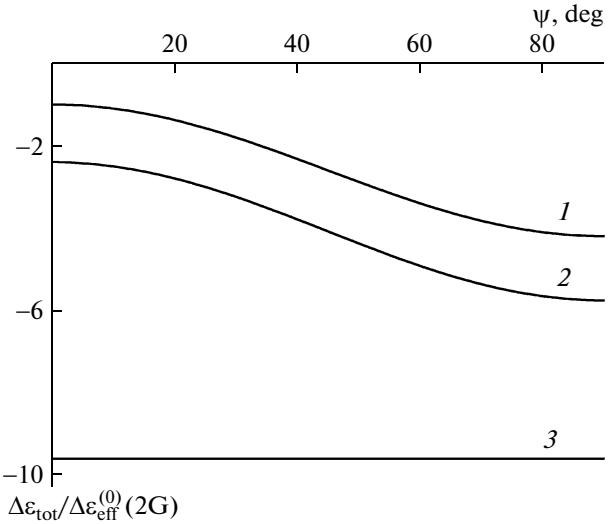

Fig. 13. Dependences of $\Delta\varepsilon_{tot}$ on rotation angle ψ of the director normalized by parameter $\Delta\varepsilon_{eff}^{(0)}$ (2G) for dendrimers of different generations: (*1*) 2G, (*2*) 3G, and (*3*) 4G. For the 4G dendrimer, parameter m defining the dependence of effective anisotropy on angle ψ is assumed to be equal to zero.

weaker. Threshold power P_1 is inversely proportional to $\Delta\varepsilon_{eff}^{(0)}$; hence, this parameter increases as the generation number increases. Figure 13 illustrates the results derived in terms of the proposed model as the dependences $\Delta\varepsilon_{tot}(\psi)$ normalized by parameter $\Delta\varepsilon_{eff}^{(0)}$ (2G).

Therefore, the theory [23] provides an adequate description of the experimentally observed orientational transitions in the NLCs during the action of light and low-frequency fields and makes it possible to gain information about parameters characterizing interaction between light and NLCs.

CONCLUSIONS

This paper has presented results on comprehensive studies of the interaction of light and low-molecular-mass nematic liquid crystals doped with high-molecular-mass compounds of diverse architectures (comb-shaped polymers and 1G–5G dendrimers) containing azobenzene fragments. The orientational optical nonlinearity induced by polymers and 2G–5G dendrimers is negative (the director rotates perpendicularly to the light field, thus decreasing the refractive index of the extraordinary light wave) in contrast to the sign-alternating nonlinearity induced by low-molecular-mass dyes whose structure is similar to that of azobenzene fragments and 1G dendrimers. The magnitude of negative nonlinearity increases as the generation number of dendrimers increases. For comb-shaped polymer P-1, the nonlinearity—to-absorption ratio exceeds corresponding values for other low-molecular-mass dyes.

The use of 2G and 3G dendrimers as dopants for the nematic matrix has for the first time made it possible to induce the first-order Freedericksz transition during the action of linearly polarized light. This transition has a broad interval of bistability. Because of the effect of light on the LC system containing dendrimers, the second-order Freedericksz transition during the action of a low-frequency field transforms into a first-order transition. The orientational first-order transitions are well described in terms of a model that takes into consideration the dependence of the factor of enhancement of nonlinearity (relative to the nonlinearity of the undoped nematic matrix) on the angle between the light field and the director.

The causes of increased nonlinearity for dopants with a more complex molecular structure require independent studies. This phenomenon can be related to changes in the order parameter of azobenzene chromophores and to the hindrance of trans–cis isomerization.

REFERENCES

1. P. G. De Gennes, *The Physics of Liquid Crystals* (Clarendon, Oxford, 1974; Mir, Moscow, 1977).
2. L. M. Blinov, *Electro-Optical and Magneto-Optical Properties of Liquid Crystals* (Nauka, Moscow, 1978; Wiley, New York, 1983).
3. I. C. Khoo and S. L. Zhuang, Appl. Phys. Lett. **37**, 3 (1980).
4. B. Ya. Zel'dovich, N. F. Pilipetskii, A. V. Sukhov, and N. V. Tabiryan, Pis'ma Zh. Eksp. Teor. Fiz. **31**, 287 (1980).

5. A. S. Zolot'ko, V. F. Kitaeva, N. Kroo, et al., Pis'ma Zh. Eksp. Teor. Fiz. **32**, 170 (1980).
6. S. M. Arakelyan and Yu. S. Chilingaryan, *Nonlinear Optics of Liquid Crystals* (Nauka, Moscow, 1984) [in Russian].
7. I. Janossy, L. Csillag, and A. D. Lloyd, Phys. Rev. A **44**, 8410 (1991).
8. I. Janossy and T. Kosa, Opt. Lett. **17**, 1183 (1991).
9. I. Janossy, Phys. Rev. E: Stat. Phys., Plasmas, Fluids, Relat. Interdiscip. Top. **49**, 2957 (1994).
10. L. Marrucci and D. Paparo, Phys. Rev. E: Stat. Phys., Plasmas, Fluids, Relat. Interdiscip. Top. **56**, 1765 (1997).
11. A. S. Zolot'ko, Pis'ma Zh. Eksp. Teor. Fiz. **68**, 410 (1998).
12. P. Palffy-Muhoray and E. Weinan, Mol. Cryst. Liq. Cryst. **320**, 193 (1998).
13. M. Warner and S. V. Fridrikh, Phys. Rev. E: Stat. Phys., Plasmas, Fluids, Relat. Interdiscip. Top. **62**, 4431 (2000).
14. I. A. Budagovsky, A. S. Zolot'ko, V. N. Ochkin, et al., Zh. Eksp. Teor. Fiz. **133**, 204 (2008).
15. M. I. Barnik, A. S. Zolot'ko, V. G. Rumyantsev, and D. B. Terskov, Kristallografiya **40**, 746 (1995).
16. I. Janossy and L. Szabados, Phys. Rev. E: Stat. Phys., Plasmas, Fluids, Relat. Interdiscip. Top. **58**, 4598 (1998).
17. A. S. Zolot'ko, A. S. Averyushkin, V. F. Kitaeva, et al., Mol. Cryst. Liq. Cryst. **451**, 41 (2006).
18. I. A. Budagovsky, A. S. Zolot'ko, N. I. Lyukhanov, et al., Zhidk. Krist. Ikh Prakt. Ispol'zov., No. 4, 22 (2006).
19. A. S. Zolot'ko, I. A. Budagovsky, V. N. Ochkin, et al., Mol. Cryst. Liq. Cryst. **488**, 265 (2008).
20. I. A. Budagovsky, V. N. Ochkin, M. P. Smayev, et al., Liq. Cryst. **36**, 101 (2009).
21. I. A. Budagovsky, V. N. Ochkin, S. A. Shvetsov, et al., Mol. Cryst. Liq. Cryst. **544**, 112 (2011).
22. E. A. Babayan, I. A. Budagovsky, A. S. Zolot'ko, et al., Kr. Soobshch. Fiz. FIAN, No. 8, 46 (2010).
23. E. A. Babayan, I. A. Budagovsky, S. A. Shvetsov, et al., Phys. Rev. E: Stat. Phys., Plasmas, Fluids, Relat. Interdiscip. Top. **82**, 061705 (2010).
24. A. Yu. Bobrovsky, A. Pakhomov, X. Zhu, et al., J. Phys. Chem. B **106**, 540 (2002).
25. A. I. Lysachkov, N. I. Boiko, E. A. Rebrov, et al., Izv. Akad. Nauk, Ser. Khim., No. 12, 2325 (2007).
26. A. S. Zolot'ko, V. F. Kitaeva, N. N. Sobolev, and A. P. Sukhorukov, Zh. Eksp. Teor. Fiz. **81**, 933 (1981).
27. V. F. Kitaeva, A. S. Zolot'ko, and M. I. Barnik, Mol. Mater. **12**, 271 (2000).
28. T. Kosa, P. Palffy-Muhoray, H. Zhang, and T. Ikeda, Mol. Cryst. Liq. Cryst. **421**, 107 (2004).
29. B. J. Frisken and P. Palffy-Muhoray, Phys. Rev. A **40**, 6099 (1989).
30. H. L. Ong, Phys. Rev. A **28**, 2393 (1983).
31. B. Ya. Zel'dovich and N. V. Tabiryan, Usp. Fiz. Nauk **147**, 633 (1985).
32. A. J. Karn, S. M. Arakelian, Y. R. Shen, and H. L. Ong, Phys. Rev. Lett. **57**, 448 (1986).
33. S.-H. Chen and J. J. Wu, Appl. Phys. Lett. **52**, 1998 (1988).
34. J. J. Wu and S.-H. Chen, J. Appl. Phys. **66**, 1065 (1989).